RAINDROP SIZE DISTRIBUTION MODELING FOR RADIO LINK DESIGN ALONG THE EASTERN COAST OF SOUTH AFRICA

T. J. O. Afullo[*]

School of Electrical, Electronic & Computer Engineering, University of KwaZulu-Natal, Durban 4041, South Africa

Abstract—A study of the raindrop size distribution along the eastern coast of South Africa (Durban) is presented. The Biweight kernel estimator based on distometer measurement is used to determine the best estimate of the measured raindrop size probability distribution function (pdf). The best kernel estimator, which results in the lowest integral square error (ISE), is used to measure the closeness of the estimated lognormal and gamma pdf of raindrop size to the measured raindrop size distribution. It is established that the optimised lognormal pdf slightly outperforms the optimised gamma pdf in terms of the mean ISE and the RMSE values, with mean ISE values of 0.026 for lognormal and 0.04 for gamma distributions, respectively, and corresponding mean RMSE values of 0.073 and 0.081, respectively. The method-of-moments gamma and lognormal distributions are observed to be worse estimators of the measured pdf than the two optimized distributions. The $N(D)$ distributions using the optimised lognormal and gamma distributions for the region are compared with those for different tropical regions, namely, India, Singapore, Nigeria, Indonesia, and Brazil. While the Indian lognormal $N(D)$ model gives the highest peak for low raindrop sizes for all rain rates, Durban's gamma and lognormal models exhibit the widest raindrop size spread over all rain rates ranging from 1–120 mm/h. Finally, the specific attenuation due to rain using the Durban models are compared against the ITU-R models and actual measurements over a 19.5 GHz LOS link; the results indicate a need for further work involving both distrometer and radio link measurements for rain rates exceeding 30 mm/h in the eastern coast of South Africa.

1. INTRODUCTION

The millimeter wave spectrum at 30–300 GHz is of great interest to service providers today because of the wide bandwidths available for communications in this frequency range. However, the greatest impediment to propagation at this frequency range is precipitation due to rainfall. Models of rain rate and raindrop size distribution are necessary for determination of attenuation due to rain. Olsen et al. [20] proposed the following formula to determine the specific attenuation due to rain:

$$A(\text{dB/km}) = kR^\alpha \tag{1}$$

Here, R is the one-minute rain rate in mm/hour, and k and α are constants that depend on frequency and wave polarization. Through the application of logarithmic regression to Mie scattering calculations, Olsen et al. derived a comprehensive set of values for the constants k and α for rain attenuation determination. The alternative approach to determining the specific rain attenuation is to derive the drop size distribution (DSD) for a given rain rate. In early experimental work, Robert Crane [7] did an extensive rain range experiment to provide a stable raindrop size distribution; his attenuation measurements and the theoretical calculations agreed to within acceptable error bounds. The specific attenuation due to rain, A, then becomes see, for example, [15]:

$$A(\text{dB/km}) = 10^{-3} \left(4.343 \int\limits_{0}^{\infty} N(D)Q_{ext}(D)dD \right) \tag{2}$$

Here, $N(D)$ is the raindrop size distribution in m^{-3}mm^{-1}, $Q_{ext}(D)$ is the extinction coefficient in mm^2, D is the raindrop diameter in mm. Since the specific attenuation can also be determined from the rain rate, R given in Equation (1) [20], the latter can be determined from the raindrop size distribution $N(D)$, raindrop terminal velocity, $v(D)$, and water density, ρ, from the relationship [3]:

$$R(\text{mm/h}) = \frac{\rho\pi}{6} \int\limits_{0}^{\infty} D^3 N(D) v(D) dD \tag{3}$$

$$v(D) = 9.65 - 10.3\exp(-0.6D)$$

The expression for $v(D)$ in (3) is an approximation due to Best [5]. The values of the terminal velocity $v(D)$ are also tabulated in Table 8.12 of Kerr [13].

The negative exponential distribution of $N(D)$ by Marshal and Palmer [16], which was developed for temperate climates, was tested by

Ajayi and Olsen [3] for Nigeria and found to overestimate the number of raindrops in the smaller and larger diameter regions. Thus the lognormal model was subsequently confirmed as the more appropriate model for tropical regions [1]. Mulangu and Afullo [18] used the Mie scattering approach and the dielectric model of Liebe to determine the extinction coefficients in (2) and, thus, the specific rain attenuation for Botswana, over the frequency range of 1–1000 GHz. Odedina and Afullo [19] determined the forward scattering amplitudes for spherical raindrops at different frequencies by using the Marshall-Palmer DSD [16], the lognormal DSD [1, 3], and the Weibull DSD [22]. However, to the author's knowledge, there has been no reported estimate of $N(D)$ for South Africa.

This paper thus focuses on determining the actual coefficients of the lognormal and gamma distributions of $N(D)$ for the eastern coast of South Africa based on distrometer measurements taken over 25 months (from October 2008 to October 2010) at the port city of Durban (29°52'S, 30°58.9'E, altitude 131 m above sea level). While the popular method of moments (MoM) is used to determine the coefficients for these distributions, in our approach, we also use the kernel estimate of the probability density function (pdf) of the raindrop size distribution. The optimum kernel estimator of the distrometer data results in the lowest error for the measured raindrop size pdf against which the other distributions are compared. The resulting values of $N(D)$ are then compared with models from other world regions. While Durban is subtropical, there is the immense maritime influence on its climate, hence the comparison of the Durban $N(D)$ with distributions from tropical regions with strong maritime influence such as Singapore, Indonesia, East coast of Brazil, and Calcutta in India — sites for which a lot of work has been reported. However, we also note that South African climate is very varied, with Cape Town having a Mediterranean climate, while Pretoria has a temperate climate; hence when we look at these two cities later, their distributions will not be compared against those of tropical areas, but rather temperate and Mediterranean regions, as corroborated by Owolawi [28].

2. MEASUREMENT AND RAIN PARAMETERS

The raindrop size measurement process involved the installation of a distrometer atop the roof of the Electrical Engineering Building, at the University of KwaZulu-Natal in Durban. The measurement system was connected to a personal computer via a data logger, as explained in the Distrometer manual [8]. The distrometer transforms the vertical momentum of an impacting drop into an electric pulse

whose amplitude is proportional to the drop diameter. A conventional pulse height analysis yields the size distribution of the rain drops. The sensor is exposed to the raindrops to be measured. Together with the processor, it produces an electric pulse for every drop hitting the membrane. In the processor RD-80, pulses are divided into 127 classes of drop size diameter, and for every drop hitting the sensor membrane, a seven-bit ASCII code is transmitted to the serial interface of the personal computer. A computer program, which is supplied with the distrometer system, is then employed to convert the data into a suitable format for recording into a file. In order to get statistically meaningful samples and to reduce the amount of data, the program reduces the number of drop classes to 20. The accuracy of the distrometer measurement is 5%.

In order to analyze the raindrop size distributions, the rain rate ranges were divided to adequately cover the four rain types in the

Table 1. Measured minutes for given rain rate ranges.

Rain Rate Range	Rain Minutes	% Total Rain Minutes
0–5 mm/h	62,281	98.14
1–5 mm/h	6,595	10.40
5–10 mm/h	783	1.23
10–20 mm/h	284	0.45
20–50 mm/h	103	0.16
50–120 mm/h	8	0.01
1 mm/h	696	1.10
3 mm/h	220	0.35
5 mm/h	156	0.25
10 mm/h	72	0.11
20 mm/h	22	0.03
30 mm/h	8	0.01
40 mm/h	5	0.01
50 mm/h	5	0.01
60 mm/h	3	0.005
66 m/h	3	0.005
76 mm/h	1	0.002
120 mm/h	1	0.002

overall distribution as per classifications of [1, 3], namely: the drizzle rain type (below 5 mm/h); the widespread rain type (5–20 mm/h); the shower rain type (20–50 mm/h); and the thunderstorm rain type (above 50 mm/h). For the above rain rate ranges, we present the corresponding plots of the raindrop size distribution. (We also note that Kumar et al. [29] have presented alternative rainfall classifications of convective and stratiform types for Singapore.) In order to account for errors due to "dead times" in the distrometer, all entries with total raindrops (summed over all 20 bins) below 10 were eliminated prior to data analysis. The total "useful" measurement data amounted to 63,459 rain minutes, out of which 98.1% were due to the drizzle rain type, 1.68% due to the widespread type, 0.16% due to the shower type, and 0.01% due to thunderstorm type (see Table 1).

We observe in Figure 1(a) that the probability density function (pdf) of raindrop size distribution for the rain type is unimodal (has only a single peak), which means that the rain type in the 0–5 mm/h rain rate range is the drizzle type alone. On the other hand, for the
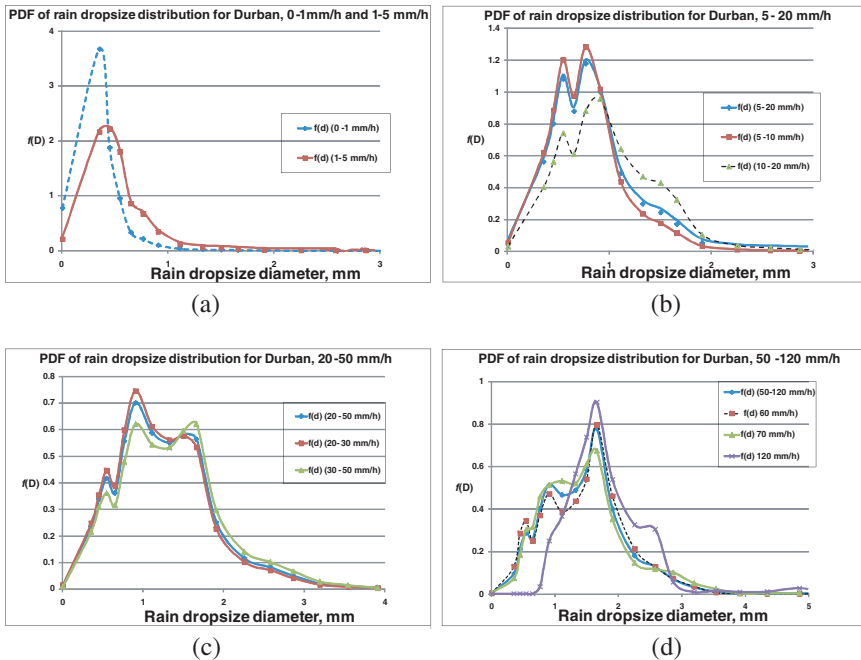

Figure 1. Probability distribution functions for selected rain rate ranges for Durban. (a) 0–5 mm/h. (b) 5–20 mm/h. (c) 20–50 mm/h. (d) 50–120 mm/h.

rain rate range 5–20 mm/h (Figure 1(b)), it is observed that the pdf is bimodal, which implies that there are now two rain types: the drizzle rain (which significantly fades off after about 10 mm/h) and the widespread rain. Further analysis for rain rate ranges 5–10 mm/h and 10–20 mm/h also display a bimodal distribution, showing that the drizzle and widespread rain types are equally dominant in the range 5–10 mm/h. However, in the range 10–20 mm/h, we observe that the widespread type is now more preponderant, with the drizzle rain type now receding. In the range 20–50 mm/h (Figure 1(c)), we observe the preponderance of the shower rain type, with the widespread peak receding at the left, and the thunderstorm peak starting to appear at the right. Finally, in the range 50–120 mm/h (in Figure 1(d)), the shower rain type has now receded as shown by the hump to the left, with the thunderstorm type being almost singularly dominant above 50 mm/h.

In order to cater for seasonal variation of raindrop size distribution, we show in Figure 2, the equivalent plots for the four
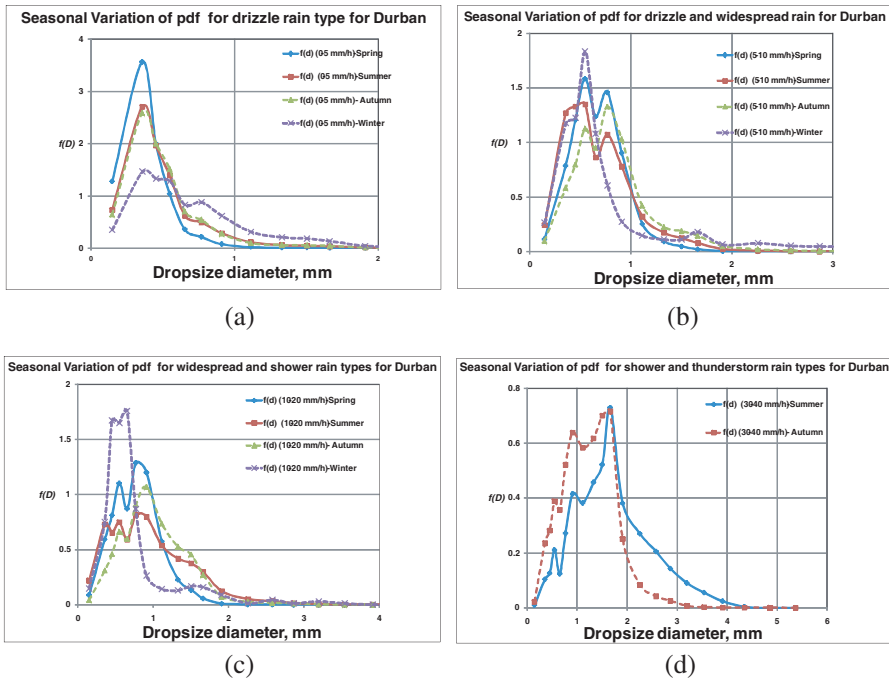

Figure 2. Seasonal variation of Probability distribution functions for selected rain rate ranges for Durban. (a) 0–5 mm/h. (b) 5–10 mm/h. (c) 10–20 mm/h. (d) 30–40 mm/h.

seasons in South Africa, namely: spring, summer, autumn, and winter. Again, these are plotted for drizzle, widespread, shower, and thunderstorm rain types. It is observed in Figure 2(a) that the raindrop size pdf remains unimodal for drizzle rain type for all seasons. However, in Figure 2(b), for the rain rate range 5–10 mm/h, the pdf is only unimodal in winter, while it is bimodal during spring, summer and autumn. In Figure 2(c), over the range 10–20 mm/h, all the distributions for the four seasons are bimodal. Note in Figure 2(d) that, there is no thunderstorm in spring and winter in Durban, but only during summer and autumn. Indeed, above 50 mm/h, where thunderstorm is the sole rain type, the only season still standing is autumn — with the pdf still bimodal. It should be noted that most of the Durban rainfall occurs during summer (October to January) and Autumn (February to March), hence the above results.

3. KERNEL ESTIMATE OF RAINDROP SIZE PDF

The estimation of raindrop size distribution, $N(D)$, is determined from Equation (15) of [26]:

$$N_T = \int_0^\infty N(D)\, dD \Rightarrow N(D) = f(D)\, N_T \tag{4}$$

Here $f(D)$ is the pdf of the raindrop size, as a function of drop diameter D (in mm), and N_T is the average of the total number of raindrops of all sizes per mm per m^3. Our approach is to use the kernel estimator to estimate $f(D)$ in (4) above. The kernel estimator, when optimised, "hugs" the actual measured $f(D)$, thus resulting in the lowest possible error. The estimate of $f(D)$, designated as $f*(D)$, for kernel K, is defined as [2, 23]:

$$f^*(D) = \frac{1}{nh} \sum_{i=1}^n K\left(\frac{D - D_i}{h}\right) \tag{5}$$

where h is the smoothing parameter, n is the sample size, D_i is the ith sample or observation of the drop size. The kernel estimator is defined as a sum of "bumps" placed at the observations: the kernel function $K(D)$ defines the shape of the bumps, while the smoothing parameter h determines the width of the bump. In this presentation, we use the *Biweight* kernel, which is defined as [23]:

$$K(D) = \begin{cases} \dfrac{15}{16}\left(1 - D^2\right)^2 & 0 \le |D| \le 1 \\ 0 & \text{elsewhere} \end{cases} \tag{6}$$

One of the most widely used measures of the global accuracy of $f*(D)$ as an estimate of $f(D)$ is the integral square error (ISE), defined as [23]:

$$\text{ISE} = \int_0^\infty [f^*(D) - f(D)]^2 \, dD \tag{7}$$

If we make the assumption that the error is uniformly distributed over the distrometer measurement range D_1 to D_2, with $f_e(D)$ the probability density function of the error, $e = [f*(D) - f(D)]$, then the RMS value of the error is determined to be:

$$\text{RMSE} = \sqrt{\int_0^\infty [f^*(D) - f(D)]^2 f_e(D) \, dD}$$

$$= \sqrt{\frac{1}{(D_2 - D_1)} \int_{D_1}^{D_2} [f^*(D) - f(D)]^2 \, dD} = \sqrt{\frac{\text{ISE}}{(D_2 - D_1)}} \tag{8}$$

The optimum h in (5) results in the minimum ISE and RMSE. In these measurements, the optimum value of h varied between 0.05 and 0.3, as the data set range, n, varied from 1,200 to 357,020. Therefore,

Table 2. Biweight kernel estimate ISE pdf for various h.

Rain Rate (mm/h)	ISE values for given h			
	$h = 0.1$	$h = 0.2$	$h = 0.3$	$h = 0.4$
1	0.0337	0.0525	0.1283	0. 2259
3	0.7421	0.0201	0.0424	0.0733
5	0.1581	0.0159	0.0235	0.0290
10	0.3716	0.0098	0.01324	0.0186
20	0.3503	0.0237	0.0116	0.0132
30	0.7746	0.0462	0.0093	0.0128
40	0.5784	0.0319	0.0092	0.0123
50	0.8393	0.0527	0.0102	0.0146
60	1.1028	0.0739	0.0080	0.0134
66	0.999	0.065	0.009	0.012
76	0.590	0.038	0.008	0.010
120	1.364	0.097	0.023	0.039

based on the above, the estimate of $f(D)$ is reported here for four values of h, namely, 0.1, 0.2, 0.3, and 0.4. For the distrometer used here, $D_1 = 0.359\,\text{mm}$, and $D_2 = 5.373\,\text{mm}$.

The pdf's as well as their kernel estimates, were determined for 12 distinct rain rates in the range 1–120 mm/h. The chosen rain rate, e.g., R_1 mm/h, covers the range $R_1 \pm 5\%$ mm/h, which was more easily accomplished for the lower rain rates, as more than 99% of the rain minutes occurred in the rain rate range below 10 mm/h. For each rain rate, the ISE and RMSE were computed, as listed in the Table 2. One observes that the optimum value of h is 0.1 for 1 mm/h, 0.2 for rain rates from 3–10 mm/h, while for 20–120 mm/h, the optimum h is 0.3. The optimised lognormal and gamma pdf's of $N(D)$ are derived next, followed by the corresponding MoM pdf's. The resulting errors (ISE and RMSE) are measured against that of the optimum kernel estimator, and thus the best lognormal and gamma estimators are defined. We therefore reiterate that the kernel estimator is specifically introduced here to provide a benchmark ISE for comparison against other derived estimators.

4. OPTIMISED LOGNORMAL AND GAMMA DSD

The lognormal $f(D)$, is related to the lognormal raindrop size distribution, $N(D)$, through the relationship:

$$N(D) = f(D)N_T = \frac{N_T}{\sigma D \sqrt{2\pi}} \exp\left[-0.5\left(\frac{\ln D - \mu_{\ln}}{\sigma_{\ln}}\right)^2\right] \qquad (9)$$

where $\mu_{\ln}$ is the mean of lnD, $\sigma_{\ln}$ is the standard deviation of lnD, and N_T is as defined above, and D is the raindrop diameter, in mm, as explained before. We first determine the variation of N_T with the rain rate, R, and obtain the following relationship for Durban:

$$N_T = A_T R^{B_T} = 369.77 R^{0.2874} \qquad 1 \le R \le 120\,\text{mm/h} \qquad (10)$$

The above relationship is determined from the rain rates given in Table 1, with N_T values obtained from the distrometer data for each rain rate. A similar relationship was obtained for the range $0 < R < 1$ mm/h. In each case, a correlation coefficient above 0.91 was obtained. In order to obtain $N(D)$, we first determine $f*(D)$ for the lognormal distribution. In this case, the initial $f*(D)$ is obtained from the raw data and, thereafter, after optimization, from the parameters giving the lowest values of ISE and RMSE. The initial estimates of the mean, $\mu_{\ln}$, and the standard deviation, $\sigma_{\ln}$, of lnD, are determined as follows, from the mean, μ, and the standard deviation, σ, of the

measured pdf (see [11]):

$$\mu_{\ln} \approx \ln(\mu) - 0.5\sigma_{\ln}^2$$
$$\sigma_{\ln} \approx \sqrt{\ln(1 + \sigma^2/\mu^2)} \tag{11}$$

The optimization process involves incrementally adjusting μ and σ about the initial estimates of Equation (11) while simultaneously observing the corresponding variation in the ISE, and continuing with the process until the lowest value of ISE is achieved. The final or optimum values of $\mu_{\ln}$ and $\sigma_{\ln}$ are obtained from this lowest ISE, which is compared with that of the original lognormal distribution, as shown in Table 3. From the table, the mean values of the ISE taken over the 12 rain rates are 0.02606 for the optimised lognormal pdf and 0.01403 for the best Biweight kernel estimator. The corresponding RMSE values are: 0.0730 and 0.0509, respectively. This thus confirms that in the process of optimization, we have been able to significantly improve on the ISE and RMSE, while still not outperforming the kernel estimator — which "hugs" the original pdf. The expressions for the lognormal distribution parameters are given as follows [4]:

$$\mu_{\ln} = A_{\mu\ln} + B_{\mu\ln}\ln(R)$$
$$\sigma_{\ln}^2 = A_{\sigma\ln} + B_{\sigma\ln}\ln(R) \tag{12}$$

Table 3. Parameters and error values for the initial and optimised lognormal distributions.

Rain Rate (mm/h)	Lognormal parameters				Optimized Lognormal parameters				Best Kernel Est.	
	$\mu_{\ln}$	$\sigma_{\ln}$	ISE	RMSE	$\mu_{\ln}$	$\sigma_{\ln}$	ISE	RMSE	ISE	RMSE
1	-0.0924	0.3681	0.1064	0.1427	-0.6197	0.3007	0.0456	0.0934	0.0337	0.0803
3	-0.3488	0.4223	0.0551	0.1027	-0.4000	0.4001	0.0445	0.0923	0.0201	0.0620
5	-0.2253	0.4099	0.0255	0.0698	-0.2200	0.4423	0.0229	0.0663	0.0159	0.0550
10	0.0139	0.4035	0.0570	0.1044	0.0600	0.4500	0.0424	0.0901	0.0098	0.0430
20	0.2034	0.4025	0.0300	0.0758	0.2586	0.4420	0.0211	0.0635	0.0116	0.0470
30	0.3843	0.4009	0.0294	0.0750	0.3981	0.4599	0.0191	0.0605	0.0093	0.0420
40	0.3737	0.4614	0.0250	0.0690	0.3743	0.4906	0.0206	0.0629	0.0092	0.0420
50	0.3989	0.182	0.0249	0.0690	0.4371	0.1835	0.0206	0.0628	0.0102	0.0442
60	0.4817	0.1450	0.0653	0.1118	0.5827	0.1906	0.0370	0.0841	0.0080	0.0391
66	0.4571	0.3617	0.0288	0.0742	0.5115	0.4139	0.0166	0.0564	0.0091	0.0416
76	0.4587	0.4707	0.0296	0.0752	0.4742	0.5509	0.0153	0.0542	0.0080	0.0391
120	0.6591	0.3304	0.04274	0.0905	0.6634	0.3224	0.0424	0.0900	0.0235	0.067

These coefficients — $A_{\mu\ln}$, $B_{\mu\ln}$, $A_{\sigma\ln}$, and $B_{\sigma\ln}$ — are determined from the optimized lognormal distribution of Table 3. The resulting coefficients from our work and other works presented in [4, 16, 21, 24, 25, 27] are shown in Table 7. The optimum lognormal coefficients obtained for the eastern coast of South Africa are:

$$\mu_{\ln} = -0.6316 + 0.2774\ln R \quad \text{for} 1 \leq R \leq 120\,\text{mm/h}$$
$$\sigma_{\ln}^2 = 0.117 + 0.0304\ln R \qquad \text{for} 1 \leq R \leq 120\,\text{mm/h} \tag{13}$$

For the three-parameter gamma distribution, the probability density function, $f(D)$, is given by:

$$f(D) = CD^{\alpha-1}\exp\left[-D/\beta\right] \tag{14}$$

where α is the shape parameter, β is the scale parameter, and C is a constant that depends on α and β, as shown in (5) below. The raindrop size distribution, $N(D)$, for the gamma distribution thus becomes [10]:

$$N(D) = f(D)N_T = N_o D^{\mu}\exp\left[-\lambda D\right];$$
$$N_o = N_T C = N_T\frac{\lambda^{\mu+1}}{\Gamma(\mu+1)};\ \mu = \alpha - 1;\ \lambda = \frac{1}{\beta} \tag{15}$$

with N_o, μ and λ expressed in terms of rain rate, R, as follows:

$$N_o = A_o R^{B_o}$$
$$\mu = A_\mu R^{B_\mu} \tag{16}$$
$$\lambda = A_\lambda R^{B_\lambda}$$

where parameters A_o, B_o, A_μ, B_μ, A_λ, and B_λ are to be determined for the region. In this work, the procedure is to determine the initial values of α, β, and C as follows: from the definition of the gamma function in (14), we use the mean, μ, and the standard deviation, σ, of the measured pdf, to determine initial gamma parameters estimates as follows:

$$\beta \approx \sigma^2/\mu;\ \alpha \approx \mu/\beta;$$
$$\int_0^{5.373} CD^{\alpha-1}\exp\left[-D/\beta\right]dD = 1 \Rightarrow C \approx \frac{1}{\int_0^{5.373} D^{\alpha-1}\exp[-D/\beta]dD} \tag{17}$$

The optimum values of α, β, and C are obtained by incrementally adjusting the values of μ and σ, about the initial values in (17) while observing the corresponding changes in ISE, until the lowest possible value of ISE is obtained, resulting in the optimum parameters of the gamma distribution. For Durban, the optimized gamma parameters

Table 4. Parameters and error values for the initial and optimised gamma distributions.

Rain Rate (mm/h)	Initial Gamma Parameters					Optimized Gamma Parameters				
	α=μ+1	β=1/λ	C	ISE	RMSE	α=μ+1	β=1/λ	C	ISE	RMSE
1	6.892	0.0866	35782	0.1718	0.1814	9.355	0.0638	1,71 0,02 5	0.1507	0.1699
3	5.123	0.1506	548.5	0.0975	0.136 6	5.692	0.1355	1178.5	0.0953	0.1351
5	5.464	0.1589	449.8	0.0318	0.0780	5.678	0.1529	585.0	0.0315	0.0777
10	5.656	0.1945	148.2	0.033 6	0.0802	5.917	0.1859	192.0	0.0334	0.0800
20	5.685	0.2338	52 .1	0.0160	0.0553	6.040	0.2200	69.2	0.0157	0.0548
30	5.736	0.2775	19 .3	0.0170	0.0571	5.137	0.3100	13.3	0.0158	0.0550
40	4.215	0.3835	6.9	0.0194	0.0613	4.041	0.4000	6.1	0.0192	0.0606
50	5.010	0.325 8	10.8	0.0196	0.0613	5.935	0.2750	18.8	0.0169	0.0569
60	6.406	0.2717	16 .5	0.0363	0.083 4	5.275	0.3300	9.0	0.0332	0.0797
66	7.156	0.235 6	30 .6	0.014 8	0.0532	6.665	0.2530	23.3	0.0143	0.0523
76	4.633	0.400	4.3	0.0492	0.0971	3.425	0.5160	3.0	0.0137	0.0512
120	8.667	0.235 5	13 .3	0.0562	0.1059	10.57 7	0.1930	25.4	0.0449	0.0946

are shown in Table 4, and the coefficients are given in Equation (18):

$$\begin{aligned} \mu &= 3.7478R^{0.1004} \\ \lambda &= 11.554R^{0.312} \\ C &= 69484R^{-2.183} \\ N_o &= 3.0\left(10^7 R^{-1.964}\right) \end{aligned} \qquad (18)$$

We therefore obtain the following mean ISE values for the gamma distribution: 0.0404 for the optimised gamma pdf and 0.01403 for best Biweight kernel estimator. The corresponding values of RMSE are 0.0805 and 0.0509, respectively. Thus we note for Durban that the optimized lognormal distribution is a slightly better estimator of the measured raindrop size pdf than the optimized gamma distribution — though both give very low errors.

5. METHOD OF MOMENTS FOR RAINDROP SIZE DISTRIBUTION

The method of moments (MoM) regression technique is a popular method for the estimation of raindrop size distribution [1, 3, 6]. The kth moment for an arbitrary $N(D)$, can be obtained from [3, 10]:

$$M_k = \int\limits_0^\infty D^k N\left(D\right) dD \qquad (19)$$

If $N(D)$ is the lognormal distribution defined in (8), then, using the third, fourth, and sixth moments (M_3, M_4, and M_6), the lognormal parameters N_T, μ and σ^2 can be estimated as [25]:

$$
\begin{aligned}
N_T &= \exp\left[\frac{1}{3}\left(24L_3 - 27L_4 + 6L_6\right)\right] \\
\mu &= \left[\frac{1}{3}\left(-10L_3 + 13.5L_4 - 3.5L_6\right)\right] \\
\lambda &= \left[\frac{1}{3}\left(2L_3 - 3L_4 + L_6\right)\right] \\
L_3 &= \ln\left(M_3\right); \quad L_4 = \ln\left(M_4\right); \quad L_6 = \ln\left(M_6\right)
\end{aligned}
\tag{20}
$$

The moments of Equation (20) were determined from the measured data, over the rain rate range 1–120 mm/h. The actual parameters for each rain rate are shown in Table 5. The corresponding values of N_T, $\mu_{\ln}$, and $\sigma_{\ln}$, for the lognormal distribution, using the MoM, are:

$$
\begin{aligned}
N_T &= 544.4R^{0.1145}, \\
\mu_{\ln} &= -0.6369 + 0.298\ln R, \\
\sigma_{\ln}^2 &= 0.2887 - 0.041\ln R,
\end{aligned}
\tag{21}
$$

Table 5. Lognormal coefficients using the Method of Moments (MoM).

| Rain Rate | Lognormal parameters from the method of moments | | | | | Best Kernel Est. | |
(mm/h)	N_T	$\mu_{\ln}$	$\sigma_{\ln}^2$	ISE	RMSE	ISE	RMSE
1	509	−0.16124	0.1964	9.6656	1.3604	0.0337	0.0803
3	605	−0.4496	0.2761	0.3287	0.2509	0.0201	0.0620
5	823	−0.64195	0.3491	0.4290	0.2866	0.0159	0.0550
10	768	−0.16124	0.1964	0.8626	0.4064	0.0098	0.0430
20	652	0.2834	0.1575	0.0836	0.1265	0.0116	0.0470
30	819	0.3522	0.1403	0.1479	0.1683	0.0093	0.0420
40	846	0.485	0.0895	0.1700	0.1804	0.0092	0.0420
45	731	0.5458	0.1688	0.0317	0.0780	0.0102	0.0442
50	639	0.6408	0.1672	0.0667	0.1129	0.0080	0.0391
60	905	0.6714	0.06375	0.1454	0.1668	0.0091	0.0416
66	1195	0.5749	0.0834	0.1010	0.1391	0.0080	0.0391
76	706	0.8314	0.0636	0.2062	0.1987	0.0235	0.067
120	1175	0.7372	0.1457	0.0698	0.1156	0.0337	0.0803

Table 6. Gamma coefficients using the Method of Moments (MoM).

Rain Rate (mm/h)	Gamma parameters from the method of moments						Best Kernel Est.	
	μ	λ	N_o	C	ISE	RMSE	ISE	RMSE
1	-2.17	1.69	417	0.34	55.13	3.2490	0.0337	0.0803
3	-0.60	2.34	2661	4.40	20.34	1.9736	0.0201	0.0620
5	-0.62	2.16	3420	4.15	21.53	2.0304	0.0159	0.0550
10	-1.01	1.56	2903	2.70	47.44	3.0139	0.0098	0.0430
20	4.71	4.26	41732	63.61	0.0478	0.0957	0.0116	0.0470
30	7.74	4.94	29691	55.13	0.0914	0.1323	0.0093	0.0420
40	5.58	3.52	7340	13.75	0.1121	0.1465	0.0092	0.0420
45	1.14	1.65	3541	4.85	0.5132	0.2591	0.0102	0.0442
50	1.20	1.53	2567	4.01	0.3509	0.1367	0.0080	0.0391
60	10.87	6.08	66300	73.24	0.0976	0.3135	0.0091	0.0416
66	7.19	4.70	54241	48.1	0.0375	0.0847	0.0080	0.0391
76	10.92	5.20	7812	11.06	0.2460	0.2169	0.0235	0.067
120	2.07	1.74	4465	3.80	0.2922	0.2365	0.0337	0.0803

The gamma distribution parameters using the method of moments are determined as follows [10, 14]:

$$G = \frac{M_4^3}{M_3^2 M_6}; \qquad \mu = \frac{11G - 8 + \sqrt{G(G+8)}}{2(1-G)}$$

$$\lambda = \frac{(\mu+4)M_3}{M_4}; \quad N_o = \frac{\lambda^{(\mu+4)} M_3}{\Gamma(\mu+4)} \tag{22}$$

Using the values of M_3, M_4, and M_6, obtained earlier, the derived gamma parameters are shown in Table 6. The values of μ and λ, N_o, and C, for the gamma distribution, using the MoM, are:

$$\mu = -2.9727 + 2.130 \ln(R)$$
$$\lambda = 1.8093 R^{0.1409}$$
$$C = 1.2107 R^{0.6462} \tag{23}$$
$$N_o = 1040 R^{0.6204}$$

Note that μ has a logarithmic rather than power law trend, due to the negative values obtained for lower rain rates of 1 to 10 mm/h.

One observes from Table 5 and Table 6 that the average ISE and RMSE values using the method of moments for the lognormal distribution are 0.947 and 0.276, respectively, compared to 0.0155 and 0.0525, respectively, for the best kernel estimator. The corresponding error values returned by the gamma distribution (using the method of moments) are even much worse, at 11.25 and 0.9145, respectively,

compared to 0.0155 and 0.0525, respectively for the best kernel estimator. Both these values are even worse than the non-optimized estimate's error values of 0.0433 and 0.0883, respectively, for the lognormal distribution, and 0.0439 and 0.1464 respectively, for the gamma distribution, as seen in Tables 3 and 4. The corresponding $N(D)$ plots are shown in Figures 3(a) to 3(d). From the figures, it is obvious that, once again, the MoM's gamma and lognormal plots fall far off the kernel plots of $N(D)$ for all rain rates, while the optimized plots are very close to it — again as expected from the relatively low values of ISE. At the higher rain rates, the problem with the two MoM distributions is that they are horizontally more offset from the real distribution, while the two optimized distributions follow the kernel $N(D)$ more closely. Thus, based on their better error performance, the two optimized lognormal and gamma distributions are adopted as the eastern coast of South Africa's models, and used to compare their performance with those from other tropical regions.
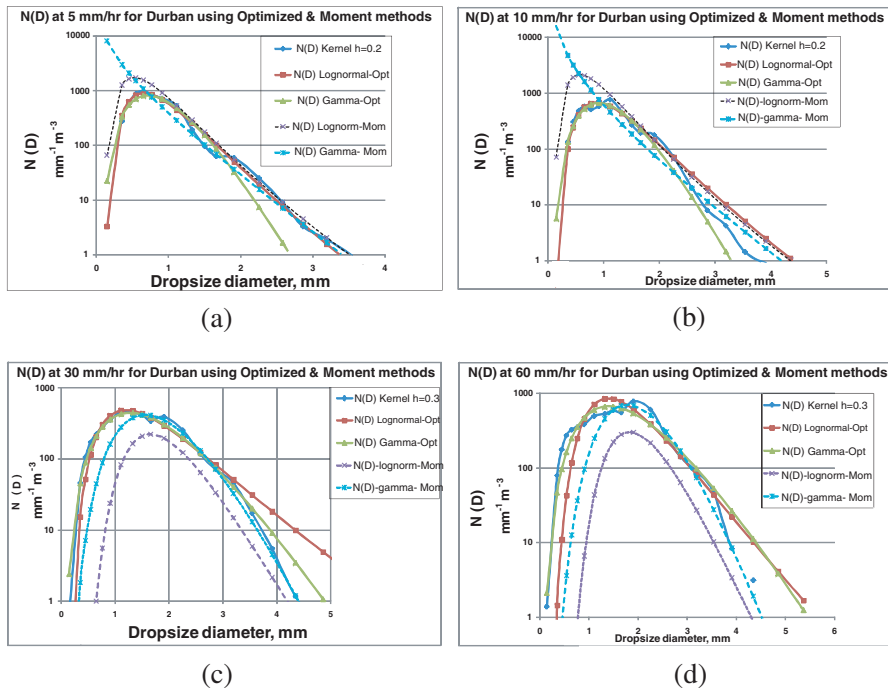

(a)

(b)

(c)

(d)

Figure 3. $N(D)$ evaluated for selected rain rates using different methods for Durban. (a) 5 mm/h. (b) 10 mm/h. (c) 30 mm/h. (d) 60 mm/h.

6. COMPARISON WITH OTHER TROPICAL RAINDROP SIZE DISTRIBUTIONS

In Figures 4(a) to 4(d), we compare the $N(D)$ plots for the eastern coast of South African with those of lognormal and gamma distributions for other tropical and sub-tropical regions, namely, Calcutta, India (22°34'N, 88°22'E), Singapore (1°21'N, 103°41'E), Ile-Ife, Nigeria (7°30'N, 4°30'E), Maceio, Brazil (9°33'S, 35°47'W), and Kototabang, Indonesia (0.20°S, 100.32°E). The lognormal distributions used in this comparison are those obtained from [15] for India, [25] for Singapore, [3, 5] for Nigeria, and [24] for Brazil. The gamma distributions used are those obtained from [17] for Indonesia, and [14, 21] for Singapore. The corresponding coefficients are shown in Table 7 and Table 8.

For all rain rates in the range 1–120 mm/h, the Indian lognormal model gives the highest peak value of $N(D)$, albeit over a very narrow
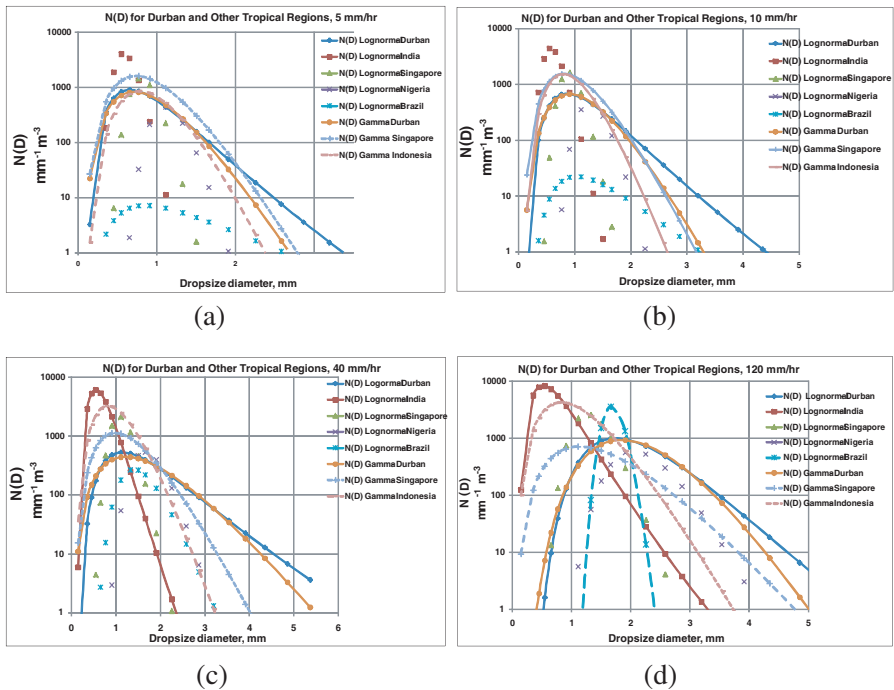

(a)

(b)

(c)

(d)

Figure 4. Comparison of $N(D)$ variations for selected rain rates in tropical regions. (a) 5 mm/h. (b) 10 mm/h. (c) 40 mm/h. (d) 120 mm/h.

Table 7. Lognormal coefficients for India, Singapore, Nigeria, Brazil, and eastern coast of South Africa.

Coefficients	India (Calcutta)	Singapore	Nigeria (Ile-Ife)	Brazil (Maceio)	South Africa (Durban)
A_T	546.00	276.18	108.00	391.00	369.77
B_T	0.4690	0.3815	0.3630	0.0090	0.2874
$A_{\mu\ln}$	-0.5380	-0.4286	-0.1950	1.5798	-0.6316
$B_{\mu\ln}$	0.0170	0.1458	0.1990	0.0145	0.2774
$A_{\sigma\ln}$	0.0689	0.1564	0.1370	2.1592	0.117
$B_{\sigma\ln}$	0.0760	0.0091	0.0130	0.0454	0.0304

Table 8. Gamma coefficients for Singapore, Indonesia, and eastern coast of South Africa.

Region	A_o	B_o	A_μ	B_μ	A_λ	B_λ
S. Africa (Durban)	3×10^7	-1.964	3.7479	0.1004	11.554	0.312
Singapore	1.038×10^7	-1.324	5.9808	-0.0981	10.0797	-0.2344
Indonesia (Kototabang)	1×10^7	-0.812	9.889	-0.179	12.85	-0.195

raindrop size range (below 1 mm diameter); it is followed by the Singaporean and Indonesian peaks, again over the entire rainfall rate range, spanning drizzle to thunderstorm rain types. As far as the spread of the distribution is concerned, the two Durban distributions exhibit the widest distribution of raindrop sizes of all five regions considered here, for all rain rates above 10 mm/h, followed by the Singaporean, Brazilian and Nigerian distributions, in that order. At low-to-medium rain rates (up to 50 mm/h), the narrowest distributions are the Indian and Singaporean lognormal distributions, while above 60 mm/h, the Brazilian and Singaporean lognormal distributions are the narrowest.

7. COMPARISONS OF SPECIFIC ATTENUATION VALUES

[20] has shown that the extinction cross-section can be related to the raindrop diameter, D, through a variation of the following expression:

$$Q_{ext}(\text{mm}^2) = \kappa \left(\frac{D}{2}\right)^{\zeta} \tag{24}$$

where κ and ζ are constants at a given frequency and temperature. [19] derived the constants κ and ζ at 20°C, for the frequency range 1–35 GHz, with Q_{ext} in cm^2. We have used slightly modified values of these parameters, also at 20°C, with Q_{ext} in mm^2, in order to determine the specific attenuation through Equation (2).

The resulting plots are shown in Figure 5(a), at $R_{0.01} = 60$ mm/h, for the $N(D)$ models for Durban, Nigeria, India, and Brazil, as well as the ITU-R models. It is observed that the two ITU-R models (representing horizontal and vertical polarizations [12]) perform close to the Durban model for frequencies above 5 GHz, with the Brazilian model also being close below 20 GHz. On the other hand, the Indian and Nigerian models consistently underestimate rain attenuation in Durban by 2–8 dB/km for frequencies above 10 GHz. In Figure 5(b), the two Durban and two ITU-R models' attenuation coefficients are compared at 20 GHz, for rain rates varying from 1–80 mm/hr, against measurements done over a 6.73-km line-of-sight link operating at 19.5 GHz in Durban, as reported by [9, 19].

Note that due to the short length of the link, the specific attenuation used here has been calculated by dividing the total attenuation over the path, A_T (dB), by the path length of 6.73 km.
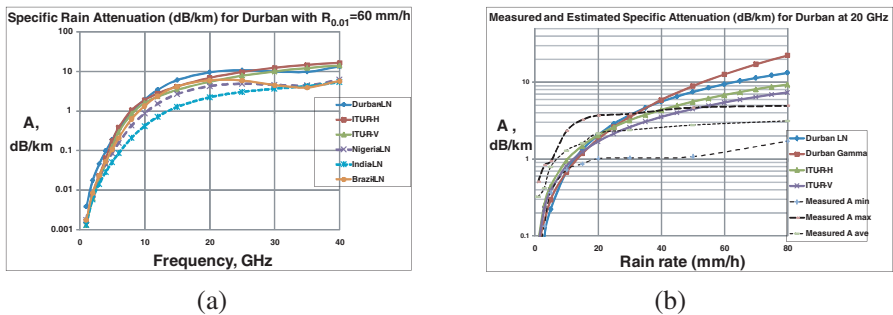

(a)   (b)

Figure 5. Comparison of Specific Rain Attenuation for Durban and selected tropical regions. (a) A (dB/km) at $R_{0.01} = 60$ mm/h. (b) Measured and Calculated A (dB/km) at 20 GHz.

While for drizzle and widespread rain types the two ITU-R models overestimate the Durban specific attenuation, above 20 mm/h, they both underestimate the specific attenuation at this frequency. The four models have their specific attenuation values falling between the minimum and maximum measured values for rain rates below 30 mm/h — which implies a reasonably good estimate of the attenuation due to rain over this rain rate range. However, above 30 mm/h, both Durban models overshoot the maximum measured attenuation, with the two ITU-R models staying within the bounds until 40–50 mm/h, when they also overshoot the measured bounds. This calls for further investigation, incorporating a longer measurement time. It is initially probable — at face value — that the rain cell size distribution, and the path reduction factor, for Durban may also need to be studied further for rain rates above 30 mm/h.

8. CONCLUSION

In this paper, we have presented results for a two-year measurement campaign using a distrometer for raindrop size distribution for Durban, on the eastern coast of South Africa. We have applied the Biweight kernel estimator on the measured distrometer data to establish the measured raindrop pdf, and determined that the kernel estimator that gives the lowest integral square error (ISE) has a smoothing parameter h in the range 0.1 to 0.3. The lognormal and gamma raindrop size distributions, $N(D)$, for the eastern coast of South Africa, are both determined via an optimization process that minimizes the ISE and the RMSE, resulting in the so-called optimised lognormal and gamma distributions. The optimized distributions are seen to outperform the MoM's lognormal and gamma distributions, giving much lower values of mean ISE and RMSE, and are thus adopted as the actual distributions for the eastern coast of South African. The resulting plots of $N(D)$ are compared with those obtained from measurements in five tropical regions, namely, India, Singapore, Nigeria, Indonesia, and Brazil. For all rain rates, the Indian (Calcutta) lognormal distribution is found to have the highest peak, while the two South African models exhibit the largest spread, thus accounting for a wider distribution of raindrop sizes for all rain rates. As far as specific attenuation is concerned, the ITU-R models for horizontal and vertical polarization are seen to perform closest to the Durban model, compared to the Indian, Nigerian, and Brazilian models at 60 mm/h. However, when compared to the actual measurements taken at 20 GHz, the two Durban models overshoot the specific attenuation bounds after 30 mm/h, thus calling for further investigation coupled

with measurements over a longer period, via the distrometer and the 20-GHz link used in this example.

ACKNOWLEDGMENT

REFERENCES

1. Adimula, I. A. and G. O. Ajayi, "Variation in raindrop size distribution and specific attenuation due to rain in Nigeria," *Ann. Telecommun.*, Vol. 51, No. 1–2, 87–93, 1996.
2. Afullo, T. J. and P. K. Odedina, "Effective earth radius factor measurement and modeling for radio link design in Botswana," *SAIEE Res. J.*, Vol. 99, No. 3, 77–86, 2008.
3. Ajayi, G. O. and R. L. Olsen, "Modeling of a tropical raindrop size distribution for microwave and millimeter wave applications," *Radio Sci. J.*, Vol. 20, No. 20, 193–202, 1985.
4. Ajayi, G. O., S. Feng, S. M. Radicella, and B. M. Reddy (eds.), *Handbook on Radiopropagation Related to Satellite Communications in Tropical and Subtropical Countries*, 2–14, ICTP Press, Trieste, 1996.
5. Best, A. C., "Empirical formulae for the terminal velocity of waterdrops falling through the atmosphere," *Quart. J. Roy Met. Soc.*, Vol. 76, 302–311, 1950.
6. Cerro, C., B. Codina, J. Bech, and J. Lorente, "Modeling raindrop size distribution and Z(R) relations in the western Mediterranean area," *Journal of Applied Meteorology*, Vol. 36, No. 11, 1470–1479, November 1997.
7. Crane, R. K., "The rain range experiment — propagation through a simulated rain environment," *IEEE Trans. Antennas & Propagation*, Vol. 22, No. 2, 321–328, March 1974.
8. Distromet System, *The Joss-Waldvogel Distrometer Handbook*, Basel, Switzerland, 2000.
9. Fashuyi, M. O. and T. J. Afullo, "Rain attenuation prediction and modeling for line-of-sight Links on terrestrial paths in South Africa," *Radio Sci. J.*, RS5006, 2007, doi: 10.1029/2007RS003618.

10. Fiser, O., M. Schonhuber, and P. Presice, "First results of DSD measurement by videodistrometer in the Czech Republic in 1998–1999," *Stud. Geophys. Geod.*, Vol. 46, 485–505, 2002.

11. Geppert: The Lognormal Distribution, Engr 323 Notes, Humboldt State University, August 15, 2011, http://www.coursehero.com/file/1763221/lognorm/.

12. ITU-R, "Specific rain attenuation model for rain for use in prediction models," *Recommend. 838-3, ITU-R P Series*, Int. Telecommun. Union, Geneva, 2005.

13. Kerr, D. E., *Propagation of Short Radio Waves,* Chapter 8, MIT Radiation laboratories Series, McGraw-Hill Book Company, 1951.

14. Kumar, L. S., Y. H. Lee, and J. T. Ong, "Truncated gamma drop size distribution models for rain attenuation in Singapore," *IEEE Trans. Ant. & Prop.*, Vol. 58, No. 4, 1325–1335, April 2010.

15. Maitra, A., "Rain attenuation modelling from measurements of rain drop size distribution in the Indian region," *IEEE Ant. & Prop. Letters*, Vol. 3, 180–181, 2004.

16. Marshall, J. S. and W. M. Palmer, "The distribution of raindrops with size," *J. Meteor.*, Vol. 5, 165–166, 1948.

17. Marzuki, M., T. Kozu, T. Shimomai, W. L. Randeu, H. Hashiguchi, and Y. Shibagaki, "Diurnal variation of rain attenuation obtained from measurement of raindrop size distribution in equatorial Indonesia," *IEEE Trans. Ant. & Prop.*, Vol. 57, No. 9, 1191–1196, April 2009.

18. Mulangu, C. T. and T. J. O. Afullo, "Variability of the propagation coefficients due to rain for microwave links in Southern Africa," *Radio Sci. J.*, RS3006, 2009, doi: 10.1029/2008RS003912.

19. Odedina, M. O. and T. J. Afullo, "Determination of rain attenuation from electromagnetic scattering by spherical raindrops: Theory and experiment," *Radio Sci. J.*, RS1003, January 27, 2010, doi:10.1029/2009RS004192.

20. Olsen, R. L., D. V. Rogers, and D. B. Hodge, "The aR^b relation in the calculation of rain attenuation," *IEEE Trans. Antennas Propag.*, Vol. 26, No. 2, 547–556, 1978.

21. Ong, J. T. and Y. Y. Shan, "Raindrop size distribution models for Singapore — comparison with results from different regions," *Proc. 10th Intl. Conf. on Ant. & Prop.*, Vol. 436, 2.281–2.285, April 14–17, 1997.

22. Sayama, S. and M. Sekine, "Influence of raindrop size distribution on the differential reflectivity up to submillimeter wavelength of 0.96 mm," *Int. J. Infrared & Millimetric Waves*, Vol. 23, No. 5,

775–784, May 2002.

23. Silverman, B. W., *Density Estimation for Statistics and Data Analysis*, Chapters 2–4, Chapman & Hall, ISBN 0-412-24620-1, 1990.

24. Tenorio, R. S, M. C. da Silva Moraes, and L. C. B. Molion, "Raindrop size distribution over north-eastern coast of Brazil," *11th URSI Open Symposium on Radio Ware Propagation & Remote Sensing*, Rio de Janeiro, Brazil, October 2007.

25. Timothy, K. I, J. T. Ong, and E. B. L. Choo, "Raindrop size distribution using method of moments for terrestrial and satellite communication applications in Singapore," *IEEE Trans. Ant. & Prop.*, Vol. 50, No. 10, 1420–1424, 2002.

26. Ulbrich, C. W., "Natural variations in the analytical form of the raindrop size distribution," *Journ. Climate & Applied Meteorology*, Vol. 22, 1764–1775, 1983.

27. Wang, M. A. and J. Din, "Comparison of the raindrop size distribution in tropical region," *Proceedings of 2004 RF and Microwave Conference*, Subang, Selangor, Malaysia, October 5–6, 2004.

28. Owolawi, P. A., "Rainfall rate probability density evaluation and mapping for the estimation of rain attenuation in South Africa and surrounding islands," *Progress In Electromagnetics Research*, Vol. 112, 155–181, 2011.

29. Kumar, L. S., Y. H. Lee, J. X. Yeo, and J. T. Ong, "Tropical rain classification and estimation of rain from Z-R (reflectivity - rain rate) relationships," *Progress in Electromagnetics Research B*, Vol. 32, 107–127, 2011.